https://doi.org/10.5194/acp-2022-483
Preprint. Discussion started: 18 July 2022

Atmospheric Chemistry and Physics Discussions

Concurrent photochemical whitening and darkening of ambient brown carbon

Qian Li[1], Dantong Liu[1*], Xiaotong Jiang[1], Ping Tian[2], Yangzhou Wu[1], Siyuan Li[1], Kang Hu[1], Quan Liu[3], Mengyu Huang[2], Ruijie Li[2], Kai Bi[2], Shaofei Kong[4], Deping Ding[2]

[1]Department of Atmospheric Science, School of Earth Science, Zhejiang University, Hangzhou, 310027, China
[2]Beijing Key Laboratory of Cloud, Precipitation and Atmospheric Water Resources, Beijing Meteorological Service, Beijing, 100089, China.
[3]State Key Laboratory of Severe Weather & Key Laboratory of Atmospheric Chemistry of CMA, Chinese Academy of Meteorological Sciences, Beijing, 100081, China
[4]Department of Atmospheric Science, School of Environmental Science, China University of Geosciences, Wuhan, 430074, China

Correspondence to: Dantong Liu (dantongliu@zju.edu.cn)

Abstract. The light-absorbing organic aerosol (OA), known as brown carbon (BrC), has important radiative impacts, however its sources and evolution after emission remain to be elucidated. In this study, the light absorption at multiple wavelengths, mass spectra of OA and microphysical properties of black carbon (BC) were characterized at a typical sub-urban environment in Beijing. The absorption of BC is constrained by its size distribution and mixing state, being subtracted from total absorption to obtain the absorption of BrC, then by applying the least-correlation of BC absorption with secondary BrC, the absorption contributed by BC, primary BrC and secondary BrC was apportioned. The multi-linear regression analysis on the factorized OA mass spectra indicated the OA from traffic and biomass burning emission contributed to primary BrC. Importantly, the moderately oxygenated OA (O/C=0.62) was revealed to highly correlate with secondary BrC. These OA had higher nitrogen content, in line with the nitrogen-containing functional groups detected by the Fourier transform infrared spectrometer. The photooxidation was found to result in reduced contribution of primary BrC about 20% but enhanced contribution of secondary BrC by 30%, implying the concurrent whitening and darkening of BrC. This provides field evidence that the photochemically produced secondary nitrogen-containing OA can considerably compensate some bleaching effect on the primary BrC, hereby causing radiative impacts.

https://doi.org/10.5194/acp-2022-483
Preprint. Discussion started: 18 July 2022

1. Introduction

Atmospheric absorbing organic aerosol (OA), known as brown carbon (BrC), is important contributor to shortwave absorption besides black carbon (BC) (Laskin et al., 2015; Liu et al., 2020), particularly at shorter visible wavelengths (Bahadur et al., 2012). Due to complex compositions of OA, the primary sources and subsequent evolution of BrC in the atmosphere remains to be explicitly understood and causes uncertainties in evaluating the radiative impacts of BrC (Liu et al., 2020).

The chromophores of BrC are mainly aromatic compounds associated with certain functional groups (Liu et al., 2015c). Particularly, compounds containing nitro, nitrated or other forms of nitrogen-containing functional groups are more absorbing (Nakayama et al., 2013; Jacobson, 1999). It is well established that primary OA, especially from biomass burning, contains a large fraction of BrC (Andreae and Crutzen, 1997; Rizzo et al., 2013; Bond, 2001). These primary BrC had a range of absorptivity, which was found to be controlled by burning phases, with OA co-emitting with BC (the flaming phase) exhibiting a higher absorptivity than OA-dominated smoldering phase (Chakrabarty et al., 2010; Saleh et al., 2014). BrC can experience reactions with atmospheric oxidants after emission. A range of field and laboratory studies found the decease of BrC absorptivity due to photobleaching on chromophores, with half decay time ranging from a few hours (Zhao et al., 2015; Liu et al., 2021) to a few days (Forrister et al., 2015), which may depend on the concentration of ambient hydroxyl radical (Wang et al., 2014). The absorptivity of BrC could be also enhanced due to addition of functional groups by forming conjugated structure with aromatics. This was supported by a number of laboratory studies that BrC absorptivity could be enhanced when forming nitrogen-containing organic compounds, such as the formation of nitro-aromatics when aromatics reacted with NO_x (Nakayama et al., 2013), or produced organic amine after reacting with ammonia (Updyke et al., 2012). The enhancement of BrC absorptivity could occur on exiting chromophores, or by producing secondary organic aerosol (SOA) through gas-phase oxidation.

The above findings mean the enhancement or bleaching of BrC absorptivity via photooxidation will coexist. The time scale between both competing processes will ultimately determine the lifetime of BrC in the atmosphere. However, both processes have been rarely investigated in the field to explicitly rule out the BrC components which principally determine the respective enhancement or decrease of its absorptivity, particularly in regions influenced by combined anthropogenic sources.

In this study, by measurements using multiple-wavelength absorption and microphysical properties of BC in a sub-urban region, the absorption of BC, primary and secondary BrC was discriminated. In conjunction with source attribution via OA mass spectra, we are able to link the segregated absorption with certain sources and investigate their primary information and subsequent evolution. The competition between photobleaching and secondary formation of BrC was investigated in real world.

2. Experimental and instrumentation

2.1 Site description and meteorology

The experiment was conducted during springtime at the Beijing Cloud Laboratory and Observational Utilities Deployment

https://doi.org/10.5194/acp-2022-483
Preprint. Discussion started: 18 July 2022

Base (117.12°E, 40.14°N), which is located in the northeast suburban area in Beijing (Fig S1a). The site is surrounded by the northwest mountain ridge, without significant local primary anthropogenic emissions (Hu et al., 2021). The 72-h backward trajectories with every 3 hours initializing from the site are analyzed by the HYSPLIT model (Draxier and Hess, 1998) using the 3-hourly 1°×1° meteorological field from the GDAS reanalysis product. The obtained backward trajectories were further clustered to group the similar transport pathways (Makra et al., 2011). The meteorological parameters, including the temperature (T) and ambient relative humidity (RH) were measured by a monitoring station on the site.

2.2 Measurements of BC microphysics and absorption coefficient

In this study, the ambient aerosol was sampled after a $PM_{2.5}$ impactor (BGI SCC 1.829) and dried by a silica drier before measurement. The single particle soot photometer (SP2, DMT., USA) was used to measure the refractory black carbon (rBC). The SP2 incandescence signal was calibrated using the Aquadag standard (Acheson Inc., USA), and a factor of 0.75 was applied to correct for ambient BC (Laborde et al., 2012). The scattering signal was calibrated by monodispersed polystyrene latex spheres (PSL). The BC core diameter (D_c) was calculated from the measured BC mass by assuming a BC density of 1.8 g cm^{-3} (Bond and Bergstrom, 2006). The leading edge only (LEO) method was applied to reconstruct the scattering signal of BC, which was used to determine the coated particle diameter (D_p) by a Mie-lookup table with the inputs of scattering and incandescence signal of each BC particle (Liu et al., 2014; Taylor et al., 2015). The mass median diameter (MMD) is derived from the D_c distribution, below and above which size the rBC mass concentration is equal (Liu et al., 2019b). The bulk coating thickness (D_p/D_c) was calculated as the cubic root of the total coated BC volume weighted by the total volume of rBC.

The mass absorption cross section (MAC) (in m^2 g^{-1}) of each BC can be calculated using the measured coated and uncoated BC sizes by applying the Mie core-shell calculation. The absorption coefficient of BC at certain wavelength, $\sigma_{abs,BC}$ (λ) is determined by multiplying the calculated MAC and rBC mass concentration at each size:

$$\sigma_{abs,BC}(\lambda)=\sum_i MAC(\lambda, D_{p,i}, D_{c,i})m(logD_{c,i})\Delta logD_{c,i} \quad (1)$$

where m ($\log D_{c,i}$) denotes the BC mass concentration at each logarithmic bin of D_c.

The absorption coefficients at wavelengths λ= 375, 470, 528, 635 and 880 nm were measured by a Micro-Aethalometer (MA200, Aethlabs, San Francisco, CA, USA). Aerosol particles were collected on filter tapes, on which the light attenuation was measured continuously with a time resolution of 30 s. The loading effect of filters was automatically corrected by measuring attenuation at two different sampling flow rates on two spots in parallel (Drinovec et al., 2015). The multiple light scattering effect was excluded by using a multi-scattering correction factor (C-value) of 3.5, 3.2 and 2.4 at the wavelengths 370 nm, 528 nm and 880 nm, respectively. It was obtained by comparing the absorption coefficient with a photoacoustic soot spectrometer (PASS-3, DMT) (Hu et al., 2021).

2.3 Attribution of primary and secondary BrC absorption

The absorption of BC at different λ is calculated using the measured uncoated core and coated size as mentioned above. The

https://doi.org/10.5194/acp-2022-483
Preprint. Discussion started: 18 July 2022

absorption of total BrC is obtained by subtracting the BC absorption from the total absorption at certain wavelength, expressed as:

$$\sigma_{abs,\,BrC}(\lambda) = \sigma_{abs,total}(\lambda) - \sigma_{abs,BC}(\lambda) \quad (2)$$

where the absorption coefficient of BC ($\sigma_{abs,BC}$) is obtained from the SP2 measurement, $\sigma_{abs,total}(\lambda)$ is the total light absorption of aerosols measured by the MA200. The absorption of secondary BrC, the absorption not contributed by primary sources, is obtained by subtracting the absorption of all primary sources from the total absorption, expressed as:

$$\sigma_{abs,secBrC}(\lambda) = \sigma_{abs,total}(\lambda) - \sigma_{abs,pri}(\lambda) \quad (3)$$

where $\sigma_{abs,pri}(\lambda)$ is the light absorption from primary sources. Here an assumption is made that light absorption from primary aerosols is all from combustion sources, and these sources necessarily contain BC (Wang et al., 2018). Therefore, the total absorption from primary sources can be obtained by scaling a factor from the mass concentration of BC, expressed as:

$$\sigma_{abs,pri}(\lambda) = \left(\frac{\sigma_{abs}}{[rBC]}\right)_{pri} \bullet [rBC] \quad (4)$$

where [rBC] is the mass concentration of rBC measured by the SP2, $\left(\frac{\sigma_{abs}}{[rBC]}\right)_{pri}$ is the scaling factor to derive the absorption of primary combustion sources from [rBC]. This factor is obtained using the minimum R-squared (MRS) approach (Wu and Yu, 2016), by adjusting the factor until a minimum correlation between $\sigma_{abs,secBrC}$ and [rBC] is reached because the absorption from secondary sources are least likely to covary with that from primary sources (Wang et al., 2019a). Being different from previous studies, an auxiliary characterization of rBC mass measured by the SP2 is used here to avoid the possible self-interference from the same measurement on absorption. The $\left(\frac{\sigma_{abs}}{[rBC]}\right)_{pri}$ ratio at λ=375 nm, 470 nm, 528 nm, 635 nm and 880 nm is calculated to be 20.7, 17.0, 14.4, 11.7 and 5, respectively (Fig. S2). This scenario assumes a relatively consistent absorption coefficient relative to BC mass concentration from sources during experiment. This however may not include some sporadic events when sources with distinct OA or BC mass fraction may be introduced and alter the single $\left(\frac{\sigma_{abs}}{[rBC]}\right)_{pri}$ ratio. The $\sigma_{abs,secBrC}$ therefore represents the overall mean value during the experimental period but this ratio will vary with seasons and locations. The σ_{abs} of primary BrC can then be calculated as:

$$\sigma_{abs,priBrC}(\lambda) = \sigma_{abs,BrC}(\lambda) - \sigma_{abs,secBrC}(\lambda) \quad (5)$$

where $\sigma_{abs,BrC}$ and $\sigma_{abs,secBrC}$ is calculated from Equation (2) and (3), respectively.

2.4 Composition measurement

The mass concentration and chemical composition of non-refractory sub-micron PM (NR-PM_1) including organic aerosols (OA), nitrate (NO_3^-), sulfate (SO_4^{2-}), chloride (Cl^-) and ammonium (NH_4^+) were determined with a High-Resolution Time-of-Flight Aerosol Mass Spectrometer (HR-ToF-AMS, Aerodyne Research Inc., USA). The setup, operation, and calibration procedures of the AMS have been described elsewhere (Canagaratna et al., 2007). During this field observation, the AMS was operated in V-mode for the quantification of mass concentrations. The composition-dependent collection efficiencies were

https://doi.org/10.5194/acp-2022-483
Preprint. Discussion started: 18 July 2022

applied (Middlebrook et al., 2012), and the ionization efficiency was calibrated using 300 nm pure ammonium nitrate (Jayne et al., 2000). Elemental ratios of OA including oxygen-to-carbon (O/C), hydrogen-to-carbon (H/C) and nitrogen-to-carbon (N/C) were determined to the improved-ambient method (Canagaratna et al., 2015).

Positive Matrix Factorization (PMF) (Paatero and Tapper, 1994) was performed on the inorganic and organic high-resolution mass spectra to distinguish OA components from different sources (Zhang et al., 2011; Ulbrich et al., 2009; Decarlo et al., 2010). The mass spectra of the combined matrix for m/z <120 were excluded in PMF analysis. Five OA factors were identified. The diagnostics of PMF is summarized in Text S1and Fig. S5.

2.5 Offline Fourier transform infrared spectrometer (FTIR) analysis

Particulate Matter (PM) samples were collected once a day onto prebaked (600°C，4h) quartz fiber filters (Whatman, QMA, USA) using a large-flow (1.05 m^3 min^{-1}) air particle sampler (TH-1000C II). The collected filter samples were stored in the refrigerator at -20°C before analysis. The infrared spectra of collected samples were measured by a Fourier transform infrared spectrometer (FTIR, Thermo Scientific, USA) equipped with an iD5 attenuated total reflectance accessory (diamond crystal) to quantify the chemical functional groups over the wavenumbers range of 550-4000 cm^{-1} with a resolution of 0.5 cm^{-1}. The NO and NO_2 symmetric stretch in the FTIR spectra can characterize the functional groups associated with nitrogen-containing organics (Coury and Dillner, 2008). Fig. S3 shows typical examples of FTIR spectra and the assigned functional groups for the three pollution levels during experiment. The peak at 1110 cm^{-1} corresponds to the background of the quartz fiber filter overlapped with some X-H bending vibrations, which is subtracted for the following analysis. The characteristic organic nitrate spectra appear at wavenumbers 860 cm^{-1} (NO symmetric stretch), 1280 cm^{-1} (NO_2 symmetric stretch) and 1630-1640cm^{-1} (NO_2 asymmetric stretch) (Bruns et al., 2010). The FTIR peaks of 1630cm^{-1} and 860cm^{-1} are integrated the absorption areas above the baseline. The summed integrated area of -NO and -NO_2 are hereby used to indicate the nitrogen-containing organics.

3. Results and Discussion

3.1 Source attributed OA

The overview results are shown in Fig. S1. The organics dominated the aerosol compositions for most time, but occasionally nitrate was the most abundant component (Fig. S1f). Note that the nitrate here may also include components containing in organics besides ammonium nitrate. Backward trajectories (Fig. S1a-d) showed that the most abundant PM_1 concentration was associated with air masses transported in shorter distance from southern regions (C1), but the longer and faster northerly transported air mass from cleaner north (C2) could dilute the concentrations.

The resolved OA factors by the PMF analysis are shown in Fig. 1, including the mass spectra, time series and diurnal profiles of each PMF factor with corresponded external tracers. Three primary OA (POA) were identified as hydrocarbon-like OA (HOA), cooking-related OA (COA), biomass burning OA (BBOA), with O/C of 0.31, 0.18 and 0.39 respectively. These POA

https://doi.org/10.5194/acp-2022-483
Preprint. Discussion started: 18 July 2022

had considerable fraction of hydrocarbon fragments (C_xH_y), indicating their less aged status. The HOA concentration correlated well with BC (r=0.62), both emitting from traffic emissions. The diurnal variation exhibited strong morning and afternoon rush-hour peaks. The OA from cooking sources (COA) had apparent fragments of both $C_4H_9^+$ and $C_3H_3O^+$, and has a higher ratio of $C_3H_3O^+/C_3H_5O^+$ (3.1), $C_4H_7^+/C_4H_9^+$ (2.2) than HOA (0.9–1.1), with a tracer fragment of $C_6H_{10}O^+$ (m/z 98) (Sun et al., 2011; Mohr et al., 2012). Its minor peak at noon and larger peak in the evening (Fig. 1l) also corresponded with the lunch and dinner time respectively.

The biomass burning OA (BBOA) was identified to contribute to about 13% of the total OA. Biomass (Cheng et al., 2013) and solid fuel burning emissions (Sun et al., 2014) have been widely observed to importantly contribute to the primary OA in this region. This off-road combustion sources were particularly abundant during wintertime for residential heating activities (Shen et al., 2019; Yang et al., 2018; Liu et al., 2016), while boiler for industry use (mostly using coal as fuel) was in operation throughout the year (Liu et al., 2015b). During the springtime of the experiment, the residential heating activities dropped due to increased ambient temperature thus the BBOA may be mainly contributed by the industry sector.

Two types of oxygenated organic aerosols (OOA) were identified, in moderate (OOA2, O/C=0.62) and high oxidation state (OOA1, O/C=0.95), respectively. The significantly higher mean OOA2 than median value in the diurnal pattern indicated that this OA type was largely associated with pollution events. Both OOA1 and OOA2 showed nighttime peak due to the dark oxidation chemistry under high relative humidity. OOA1 showed particularly high correlation with sulfate (r=0.40) because of their similar volatilities (Huffman et al., 2009; Jimenez et al., 2009). The slight enhancement at noon for OOA1 (also for OOA2) soon after morning rush-hour indicated the likely rapid formation of SOA through photooxidation. Notably, OOA2 had a substantially higher N/C than other factors (N/C=0.037), and had highest correlation with nitrate (r=0.77) and with $C_xH_yN_z$ and $C_xH_yN_zO_p$ fragments (r=0.83). This factor therefore tends to largely result from nitrogen-containing OA.

https://doi.org/10.5194/acp-2022-483
Preprint. Discussion started: 18 July 2022

Atmospheric Chemistry and Physics Discussions

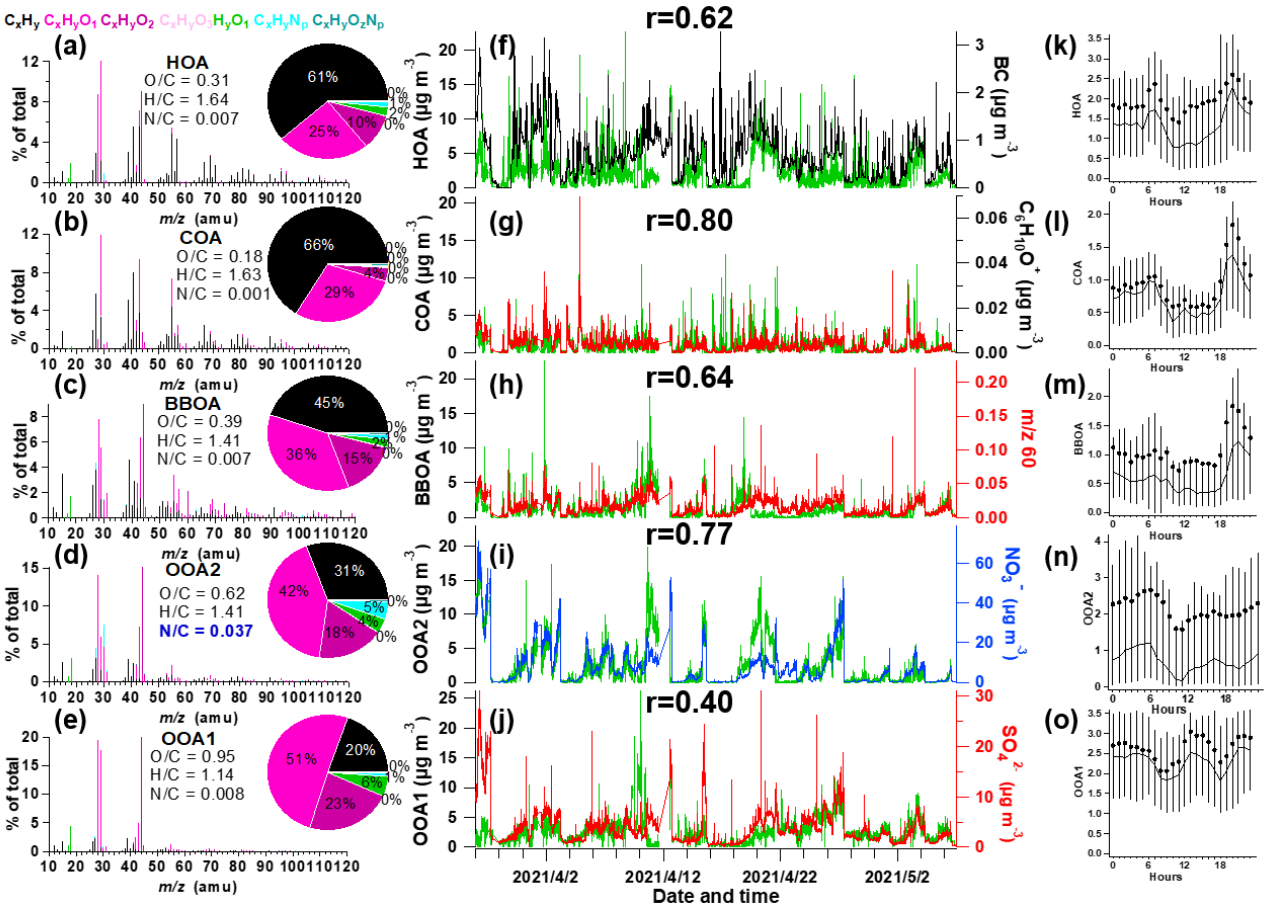

Figure 1. Information of source-apportioned organic aerosols by the PMF analysis. Mass spectra of (a) hydrocarbon-like OA (HOA), (b) cooking-related OA (COA), (c) biomass burning OA (BBOA), (d) oxygenated OA2 (OOA2), (e) oxygenated OA1 (OOA1). (f-j) Temporal variations of each PMF factor and the corresponding marker species. (k-o) Diurnal profiles of each factor. The lines, dots and whiskers denote the median, mean and the 25th/75th percentiles at each hour respectively.

3.2 Segregated aerosol absorption

Fig. 2 shows the time series of BC properties, including the BC mass concentration, D_p/D_c, D_c, MAC and light absorption of BC (section 2.2). The MMD of BC core varied between 93 – 274 nm which may correspond to the source-specific information (Liu et al., 2019a) or coagulation process during ageing. The coating of BC (indicated by D_p/D_c) showed sporadic enhancement which was closely associated with enhanced PM concentration (Fig. 2a). This was consistent with previous studies that high coatings of BC occurred during heavier pollution due to the enhanced secondary formation of condensable materials to particle phase (Ding et al., 2019; Zhang et al., 2018). This clearly indicates the variation of mixing state of BC and this will potentially influence its MAC and absorption Ångström exponent (AAE) (Liu et al., 2015a). It will introduce considerable uncertainties to use consistent MAC or AAE to derive the absorption of BC at multiple wavelengths. The calculated MAC using the measured BC core size and coatings (Fig. 2c) is thus used to derive the $\sigma_{abs,BC}$ (section 2.2, shown in Fig. 2d). MAC of BC at

https://doi.org/10.5194/acp-2022-483
Preprint. Discussion started: 18 July 2022

λ=375nm is showed to be at 8.4 -16.6 m^2 g^{-1} with enhanced absorption when high coatings.

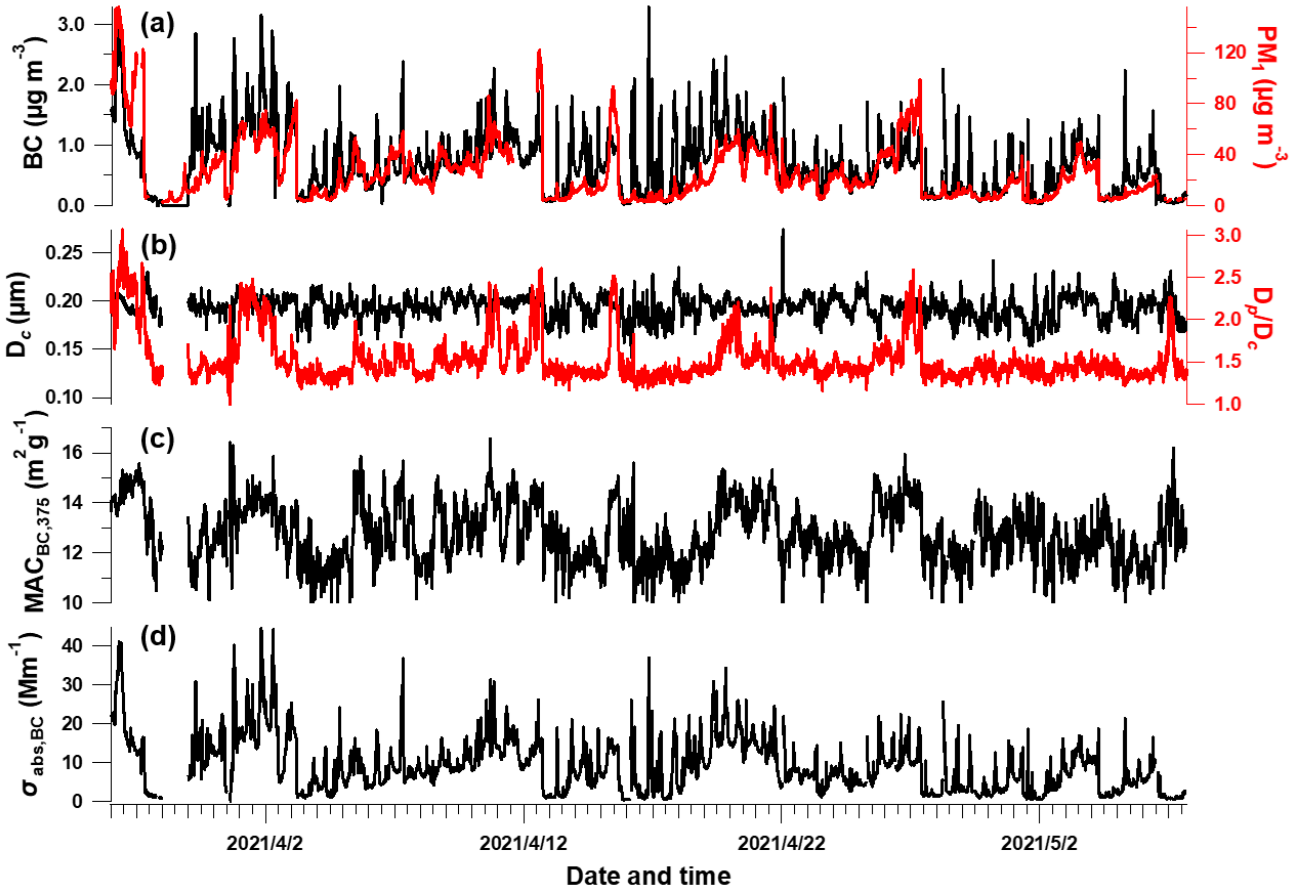

Figure 2. Temporal evolution of BC-related properties. (a) rBC and PM_1 mass concentration, (b) BC core diameter and bulk coating thickness (D_p/D_c), (c) calculated mass absorption cross section (MAC) at λ=375nm, (d) absorption coefficient of BC.

Using the calculated $\sigma_{abs,BC}$ above, the derived σ_{abs} for primary and secondary BrC (section 2.3) at λ=375nm is shown in Fig. 3b-c. In Fig. 3b, the brown and green shades above the adjacent tracer indicate the σ_{abs} of primary and all aerosols, respectively. Fig. 3c shows that $\sigma_{abs,priBrC}$ is higher than $\sigma_{abs,secBrC}$ for most time, but for certain periods they are equivalent or secondary BrC occasionally exceeds. The mean contribution of absorption for BC, primary BrC and secondary BrC is 50.8%, 27.4% and 21.8% in this study. The tracers associated with nitrogen-containing organics, such as OOA2 (with highest N/C), $C_xH_yN_z$ and $C_xH_yN_zO_p$ fragments and FTIR measured -NO + -NO_2 bond vibration, are also shown in Fig. 3d-e.

https://doi.org/10.5194/acp-2022-483
Preprint. Discussion started: 18 July 2022

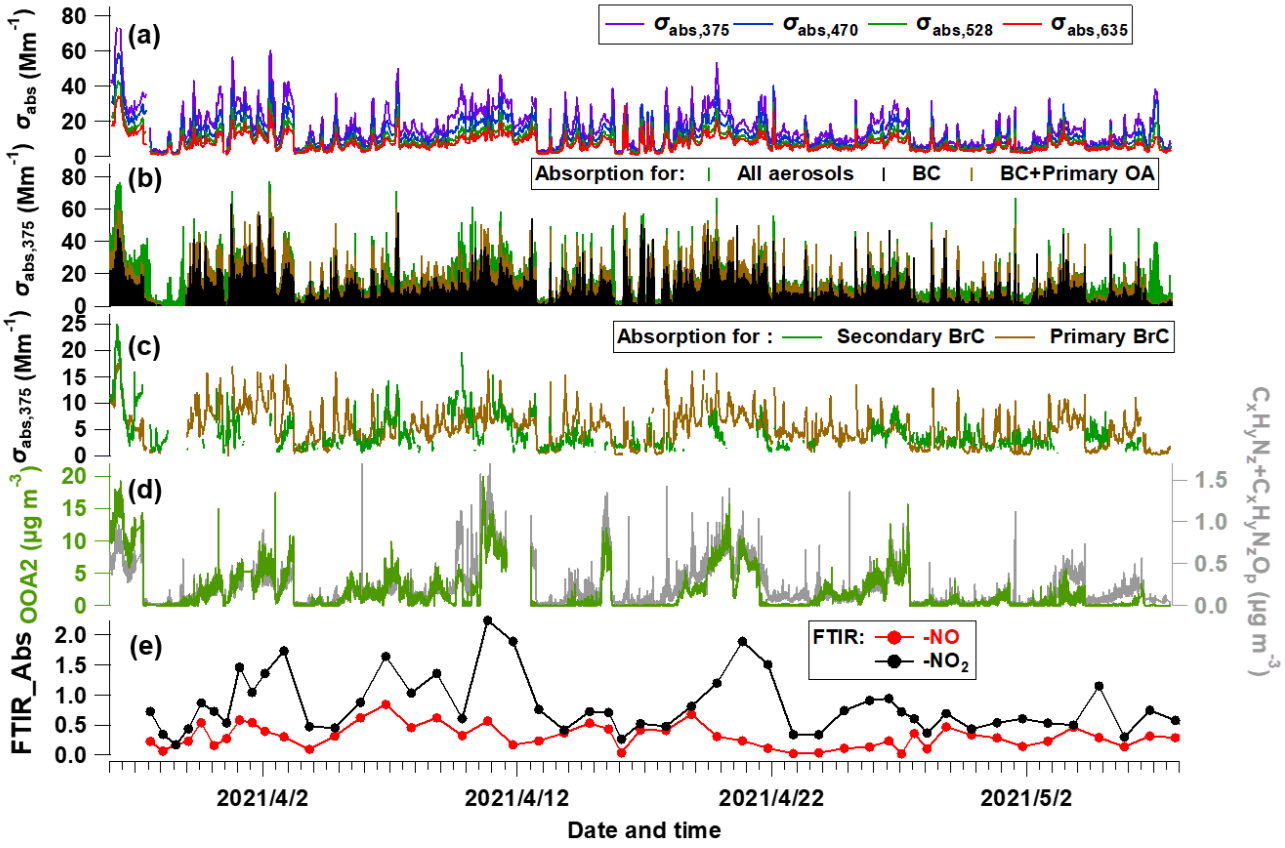

Figure 3. Temporal evolution of segregated absorbing properties. (a) Absorbing coefficients (σ_{abs}) at multiple wavelengths measured by the aethalometer, (b) σ_{abs} at λ=375nm ($\sigma_{abs,375}$) for all aerosols, primary OA and BC, (c) $\sigma_{abs,375}$ for primary BrC and secondary BrC. (d) mass concentration of OOA2 and the $C_xH_yN_z$ and $C_xH_yN_zO_p$ fragments measured by the AMS. (e) FTIR-measured absorption of -NO and -NO_2 bonds.

3.3 Source attribution of BrC absorption

A multiple linear regression (MLR) analysis is performed to apportion the absorption coefficient of BrC with the PMF attributed OA factors, expressed as:

$$\sigma_{abs,BrC}=a_0+a_1\bullet[OOA1]+a_2\bullet[OOA2]+a_3\bullet[BBOA]+a_4\bullet[COA]+a_5\bullet[HOA] \quad (6)$$

where a_0 to a_5 represents the regression coefficients for each factor. The contribution of each source-specific OA factor to $\sigma_{abs,BrC}$ can be obtained. This analysis is performed for the total BrC, primary and secondary BrC respectively. The results are shown in Table 1. MLR on the total BrC shows high correlation (r>0.4) with the factors of HOA, BBOA and OOA2, suggesting the potential importance of the primary biomass burning and traffic source, in addition to OOA2 in contributing to the absorption of BrC. MLR analysis on the primary BrC distinguishes its high correlation with BBOA (r=0.40) and HOA (r=0.46), while MRL on the secondary BrC has a high correlation with OOA2 only (r=0.44). The MRL analysis links the apportioned absorption by measurements of physical properties with source-attributed chemical compositions, therefore validating and

https://doi.org/10.5194/acp-2022-483
Preprint. Discussion started: 18 July 2022

identifying the sources of primary and secondary BrC.

Table 1. Results of the multilinear regression analysis (MLR) between $\sigma_{abs,375}$ and the five PMF-resolved OA factors, with $\sigma_{abs,375}$ of total BrC, primary and secondary BrC as dependent, respectively. All regression coefficients have passed the significance test with p<0.01. Partial correlations above 0.4 are marked in red. Since negative values appear when the COA participates, which is thus not included in the final regression but the values using COA factor are shown in brackets.

Dependent	$\sigma_{abs,BrC}$		$\sigma_{abs,pri\ BrC}$		$\sigma_{abs,sec\ BrC}$	
Model	**Regression coefficient**	**Partial correlation**	**Regression coefficient**	**Partial correlation**	**Regression coefficient**	**Partial correlation**
Constant	2.26		1.67		1.47 (1.52)	
OOA1	0.57	0.23	0.04	0.02	0.46(0.46)	0.24 (0.24)
OOA2	1.22	**0.53**	0.37	0.25	0.74 (0.74)	**0.44 (0.44)**
BBOA	2.59	**0.46**	1.22	**0.40**	1.14 (1.18)	0.29 (0.29)
COA	1.30	0.22	1.45	0.36	/ (-0.25)	/ (-0.05)
HOA	1.70	**0.47**	1.17	**0.46**	0.49 (0.52)	0.20 (0.21)
R^2	0.77		0.63		0.55 (0.55)	

Importantly, an oxygenated secondary OA factor (OOA2) is identified to significantly contribute to the secondary BrC. This OOA has a moderate O/C (0.62) and a highest N/C of 0.037 among all factors. The high N/C means this factor contains the most abundant nitrogen-containing fragments, implied as its high correlation with the $C_xH_yN_z$ and $C_xH_yN_zO_p$ fragments (r=0.83, Fig. 3d) and with the FTIR absorption for -NO_2 and -NO bonds (r=0.69, Fig. S4). The -NO bond is mostly related to the organic nitrates ($RONO_2$), and -NO_2 peak could result from both organic nitrates and nitro-organics (Bruns et al., 2010). There is no discernable peak for organic amines. These all consistently imply that the OOA2 factor contained substantial fraction of nitrogen-containing organics, and these compounds have contributed to the absorption of secondary BrC.

3.4 Simultaneous whitening and darkening process of BrC

The diurnal variation of $\sigma_{abs,375}$ for BC and primary BrC showed consistent morning rush-hour peaks at 6:00-8:00 and the night-time enhancement due to reduced boundary layer. This was in line with the morning peak of HOA and night peak of BBOA. The traffic source in this region, in particular the diesel vehicles, was reported to emit considerable OA with certain chromophores, such as aromatics (Yao et al., 2015) and heterocyclic organic compounds (Gentner et al., 2017; Schuetzle, 1983). In the morning rush-hour, BC and primary BrC occupied 51±4% and 29±4% in the total $\sigma_{abs,375}$ respectively, with the remaining 20±2% classified as secondary BrC. The night had contributions from BC and primary BrC at 50±2% and 30±3% respectively, with 20±3% as secondary BrC. Fig. 4b showed the decrease of primary BrC absorption tended to be more rapid than the HOA and BBOA mass (even a slight increase for HOA), which indicated the likely photobleaching process causing

https://doi.org/10.5194/acp-2022-483
Preprint. Discussion started: 18 July 2022

the decreased absorption efficiency per unit mass for primary BrC. This is consistent with a recent chamber study that the primary BrC could be bleached to half of the initial absorptivity in 2-3 hours for biomass burning plumes (Liu et al., 2021). Besides the morning rush-hour peak, there was an early afternoon peak for the absorption of secondary BrC, prevailing the dilution effect of daytime boundary layer (Fig. 4c). The night and morning peak of OOA2 and the morning peak of $\sigma_{abs,secBrC}$ may result from primarily emitted moderately oxygenated OA, which was reported from some diesel sources (Dewitt et al., 2015; Gentner et al., 2012). The fraction of secondary BrC thus had a pronounced early afternoon peak soon after the peak solar radiation (Fig. 4g) and a peak after midnight soon after the nighttime peak of primary BrC (Fig. 4f). This shift of peaking time from primary to secondary BrC demonstrates the likely process of SOA formation from gases, and these SOA compounds containing nitrogen (i.e., the OOA2) considerably contributed to the light absorption. This ageing or oxidation occurred at early afternoon through photooxidation or likely aqueous processes at nighttime when high RH (Fig. 4h). The oxidized volatile organic compounds (VOCs) with nitrogen chemistry involved could condense to produce additional mass in particle phase (Ehn et al., 2014; Finewax et al., 2018). Due to the high NO_x emission, photooxidation of traffic VOCs may have largely involved nitrogen chemistry. Previous studies found the NO_x-involved SOA could produce considerable chromophores (Lin et al., 2015; Siemens et al., 2022), such as the traffic VOCs may produce SOA in a time scale of hours, containing nitro-aromatics (Wang et al., 2019b; Keyte et al., 2016). The daytime formation of organic nitrate may follow the gas-phase photooxidation mechanism, in which the excess NO could add to the peroxy radical to produce organic nitrate (Liebmann et al., 2019). The nighttime chemistry involving NO_3 through the oxidation of NO_2 by O_3, contributed to the important formation of organic nitrate by initializing the production of nitrooxy peroxy radicals (Ng et al., 2008; Rollins et al., 2012). Laboratory studies (Nakayama et al., 2013; Liu et al., 2015c) also widely observed the rapid production of nitrogen-containing OA involving NO_x chemistry could contribute to light absorption of aerosols.

Overall, by apportioning the absorption of primary and secondary BrC, we found the photooxidation led to an enhanced contribution of secondary BrC by 30% but reduced contribution of primary BrC about 20% in the semi-urban environment. This revealed that the whitening and darkening of BrC had simultaneously, and the secondary BrC produced by photooxidation may compensate some bleaching effect of primary BrC. The dominance of both competing processes may depend on the timescale and location in the atmosphere. For example, the enhanced BrC fraction observed above the planetary boundary layer may be explained by the enhanced secondary BrC (Tian et al., 2020), while further ageing may bleach the produced chromophores of these SOA.

https://doi.org/10.5194/acp-2022-483
Preprint. Discussion started: 18 July 2022

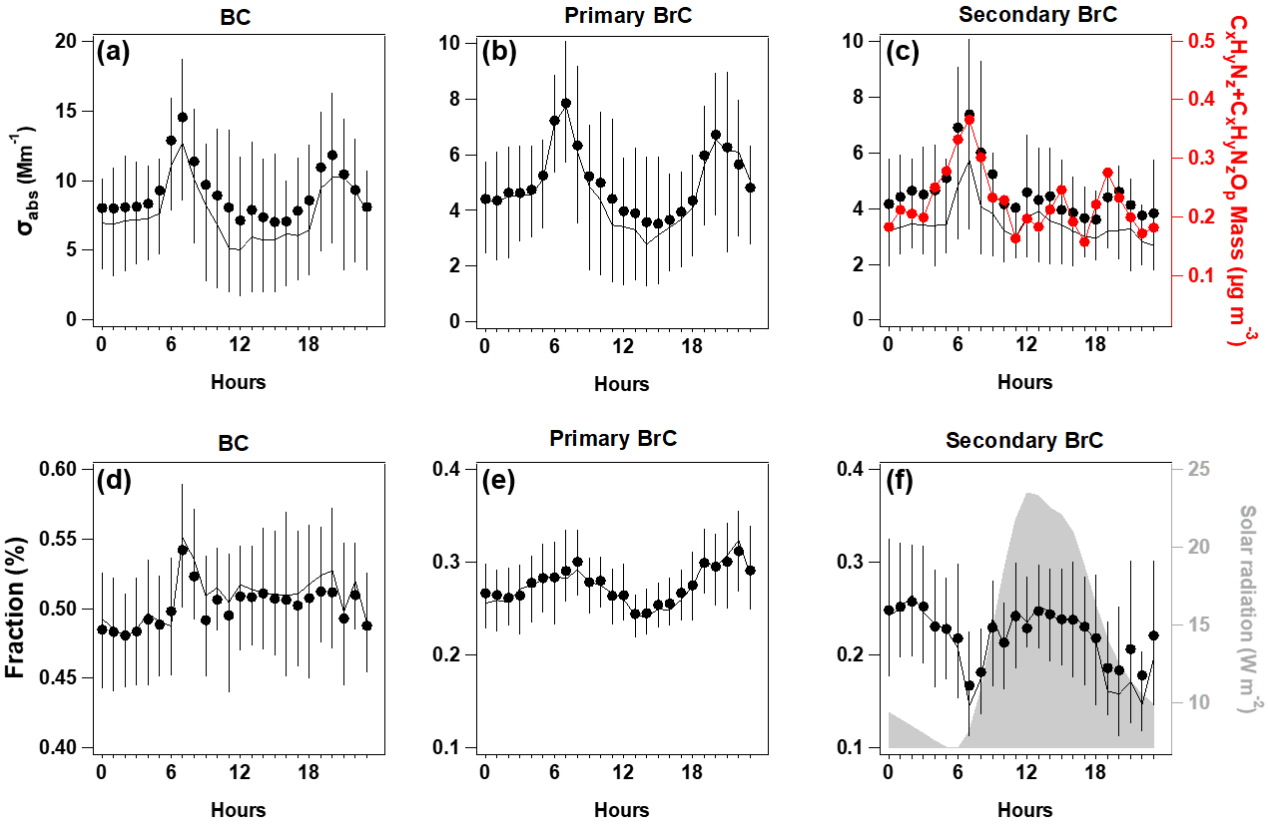

Figure 4. Diurnal variations of absorption coefficient at λ=375nm ($\sigma_{abs,375}$) for BC (a), primary BrC (b), and secondary BrC (c), along with the $C_xH_yN_z$ and $C_xH_yN_zO_p$ fragments; the respective fraction in total for the segregated $\sigma_{abs,375}$ (d-f), with direct radiation shown in shade. In each plot, the lines, dots and whiskers denote the median, mean and the 25th/75th percentiles at each hour respectively.

4. Conclusion

This study apportioned the shortwave absorption of BC, primary and secondary BrC, through concurrent measurements of BC microphysical properties and OA mass spectra. The apportioned primary BrC absorption was linked with traffic and biomass burning emissions, while secondary BrC was found to be associated with an oxygenated secondary OA factor with higher nitrogen content. The enhancement of secondary BrC and decease of primary BrC simultaneously occurred via daytime photooxidation. The results emphasize the importance of nitrogen-containing OA in contributing to BrC. These OA could primarily emit as aerosol phase, or in gas phase which requires further oxidation to be in aerosol phase to serve as BrC. The NO_x-involved chemistry is prone to add nitrogen element to the existing OA and enhance the absorptivity of chromophores. The anthropogenic NO_x emission could be therefore an important source in producing shortwave absorbing components in the atmosphere, which may offset some of the conventionally-thought photobleaching of BrC.

https://doi.org/10.5194/acp-2022-483
Preprint. Discussion started: 18 July 2022

Atmospheric Chemistry and Physics Discussions

Acknowledgments

This research was supported by the National Natural Science Foundation of China (Grant No. 42175116 and 41875167), National Key R&D Program of China (2019YFC0214703).

Author contribution

D.L., X.J. and Qian L. prepared and designed the observation. D.L., Qian L., X.J and P.T. initiated the field campaign and conducted the measurements. Qian L., D.L. P.T., Y.W., S.L. and K.H. contributed to the data analysis. Quan L., H.M., L.R., B.K., D.D. and S.K. provided technical support and assistance. Qian L. and D.L. wrote the manuscript. All authors read and approved the final manuscript.

https://doi.org/10.5194/acp-2022-483
Preprint. Discussion started: 18 July 2022

References

Andreae, M. O. and Crutzen, P. J.: Atmospheric aerosols: Biogeochemical sources and role in atmospheric chemistry, Science, 276, 1052-1058, doi:10.1126/science.276.5315.1052, 1997.

Bahadur, R., Praveen, P. S., Xu, Y., and Ramanathan, V.: Solar absorption by elemental and brown carbon determined from spectral observations, Proceedings of the National Academy of Sciences of the United States of America, 109, 17366-17371, doi:10.1073/pnas.1205910109, 2012.

Bond, T. C.: Spectral dependence of visible light absorption by carbonaceous particles emitted from coal combustion, Geophysical Research Letters, 28, 4075-4078, doi:10.1029/2001gl013652, 2001.

Bond, T. C. and Bergstrom, R. W.: Light absorption by carbonaceous particles: An investigative review, Aerosol Science and Technology, 40, 27-67, doi:10.1080/02786820500421521, 2006.

Bruns, E. A., Perraud, V., Zelenyuk, A., Ezell, M. J., Johnson, S. N., Yu, Y., Imre, D., Finlayson-Pitts, B. J., and Alexander, M. L.: Comparison of FTIR and Particle Mass Spectrometry for the Measurement of Particulate Organic Nitrates, Environmental Science & Technology, 44, 1056-1061, 10.1021/es9029864, 2010.

Canagaratna, M. R., Jimenez, J. L., Kroll, J. H., Chen, Q., Kessler, S. H., Massoli, P., Hildebrandt Ruiz, L., Fortner, E., Williams, L. R., Wilson, K. R., Surratt, J. D., Donahue, N. M., Jayne, J. T., and Worsnop, D. R.: Elemental ratio measurements of organic compounds using aerosol mass spectrometry: characterization, improved calibration, and implications, Atmospheric Chemistry and Physics, 15, 253-272, doi:10.5194/acp-15-253-2015, 2015.

Canagaratna, M. R., Jayne, J. T., Jimenez, J. L., Allan, J. D., Alfarra, M. R., Zhang, Q., Onasch, T. B., Drewnick, F., Coe, H., Middlebrook, A., Delia, A., Williams, L. R., Trimborn, A. M., Northway, M. J., DeCarlo, P. F., Kolb, C. E., Davidovits, P., and Worsnop, D. R.: Chemical and microphysical characterization of ambient aerosols with the aerodyne aerosol mass spectrometer, Mass Spectrometry Reviews, 26, 185-222, doi:10.1002/mas.20115, 2007.

Chakrabarty, R. K., Moosmueller, H., Chen, L. W. A., Lewis, K., Arnott, W. P., Mazzoleni, C., Dubey, M. K., Wold, C. E., Hao, W. M., and Kreidenweis, S. M.: Brown carbon in tar balls from smoldering biomass combustion, Atmospheric Chemistry and Physics, 10, 6363-6370, doi:10.5194/acp-10-6363-2010, 2010.

Cheng, Y., Engling, G., He, K. B., Duan, F. K., Ma, Y. L., Du, Z. Y., Liu, J. M., Zheng, M., and Weber, R. J.: Biomass burning contribution to Beijing aerosol, Atmospheric Chemistry and Physics, 13, 7765-7781, doi:10.5194/acp-13-7765-2013, 2013.

Coury, C. and Dillner, A. M.: A method to quantify organic functional groups and inorganic compounds in ambient aerosols using attenuated total reflectance FTIR spectroscopy and multivariate chemometric techniques, Atmospheric Environment, 42, 5923-5932, doi:10.1016/j.atmosenv.2008.03.026, 2008.

DeCarlo, P. F., Ulbrich, I. M., Crounse, J., de Foy, B., Dunlea, E. J., Aiken, A. C., Knapp, D., Weinheimer, A. J., Campos, T., Wennberg, P. O., and Jimenez, J. L.: Investigation of the sources and processing of organic aerosol over the Central Mexican Plateau from aircraft measurements during MILAGRO, Atmospheric Chemistry and Physics, 10, 5257-5280, doi:10.5194/acp-10-5257-2010, 2010.

DeWitt, H. L., Hellebust, S., Temime-Roussel, B., Ravier, S., Polo, L., Jacob, V., Buisson, C., Charron, A., Andre, M., Pasquier, A., Besombes, J. L., Jaffrezo, J. L., Wortham, H., and Marchand, N.: Near-highway aerosol and gas-phase measurements in a high-diesel environment, Atmospheric Chemistry and Physics, 15, 4373-4387, doi:10.5194/acp-15-4373-2015, 2015.

Ding, S., Liu, D., Zhao, D., Hu, K., Tian, P., Zhou, W., Huang, M., Yang, Y., Wang, F., Sheng, J., Liu, Q., Kong, S., Cui, P., Huang, Y., He, H., Coe, H., and Ding, D.: Size-Related Physical Properties of Black Carbon in the Lower Atmosphere over Beijing and Europe, Environmental Science & Technology, 53, 11112-11121, doi:10.1021/acs.est.9b03722, 2019.

Draxier, R. R. and Hess, G. D.: An overview of the HYSPLIT_4 modelling system for trajectories, dispersion and deposition, Australian Meteorological Magazine, 47, 295-308, 1998.

Drinovec, L., Mo?Nik, G., Zotter, P., Prév?t, A. S. H., Ruckstuhl, C., Coz, E., Rupakheti, M., Sciare, J., Müller, T., and Wiedensohler, A.: The "dual-spot" Aethalometer: an improved measurement of aerosol black carbon with real-time loading compensation, Atmospheric Measurement Techniques, 8, 1965-1979, 2015.

Ehn, M., Thornton, J. A., Kleist, E., Sipila, M., Junninen, H., Pullinen, I., Springer, M., Rubach, F., Tillmann, R., Lee, B., Lopez-Hilfiker, F., Andres, S., Acir, I.-H., Rissanen, M., Jokinen, T., Schobesberger, S., Kangasluoma, J., Kontkanen, J., Nieminen, T., Kurten, T., Nielsen, L. B., Jorgensen, S., Kjaergaard, H. G., Canagaratna, M., Dal Maso, M., Berndt, T., Petaja, T., Wahner, A., Kerminen, V.-M., Kulmala, M., Worsnop, D. R., Wildt, J., and Mentel, T. F.: A large source of low-volatility secondary organic aerosol, Nature, 506, 476-+, doi:10.1038/nature13032, 2014.

Finewax, Z., de Gouw, J. A., and Ziemann, P. J.: Identification and Quantification of 4-Nitrocatechol Formed from OH and NO3 Radical-Initiated Reactions of Catechol in Air in the Presence of NOx: Implications for Secondary Organic Aerosol Formation from Biomass Burning, Environmental Science & Technology, 52, 1981-1989, doi:10.1021/acs.est.7b05864, 2018.

Forrister, H., Liu, J., Scheuer, E., Dibb, J., Ziemba, L., Thornhill, K. L., Anderson, B., Diskin, G., Perring, A. E., Schwarz, J. P., Campuzano-Jost, P., Day, D. A., Palm, B. B., Jimenez, J. L., Nenes, A., and Weber, R. J.: Evolution of brown carbon in wildfire plumes, Geophysical Research Letters, 42, 4623-4630, doi:10.1002/2015gl063897, 2015.

Gentner, D. R., Isaacman, G., Worton, D. R., Chan, A. W. H., Dallmann, T. R., Davis, L., Liu, S., Day, D. A., Russell, L. M., Wilson, K. R., Weber, R., Guha, A., Harley, R. A., and Goldstein, A. H.: Elucidating secondary organic aerosol from diesel and gasoline vehicles through detailed characterization of organic carbon emissions, Proceedings of the National Academy of Sciences of the United States of America, 109, 18318-18323, doi:10.1073/pnas.1212272109, 2012.

Gentner, D. R., Jathar, S. H., Gordon, T. D., Bahreini, R., Day, D. A., El Haddad, I., Hayes, P. L., Pieber, S. M., Platt, S. M., de Gouw, J., Goldstein, A. H., Harley, R. A., Jimenez, J. L., Prevot, A. S. H., and Robinson, A. L.: Review of Urban Secondary Organic Aerosol Formation from Gasoline and Diesel Motor Vehicle Emissions, Environmental Science & Technology, 51, 1074-1093, doi:10.1021/acs.est.6b04509, 2017.

Hu, K., Liu, D., Tian, P., Wu, Y., Deng, Z., Wu, Y., Zhao, D., Li, R., Sheng, J., Huang, M., Ding, D., Li, W., Wang, Y., and Wu, Y.: Measurements of the Diversity of Shape and Mixing State for Ambient Black Carbon Particles, Geophysical Research Letters, 48, doi:10.1029/2021gl094522, 2021.

Huffman, J. A., Docherty, K. S., Aiken, A. C., Cubison, M. J., Ulbrich, I. M., DeCarlo, P. F., Sueper, D., Jayne, J. T., Worsnop,

D. R., Ziemann, P. J., and Jimenez, J. L.: Chemically-resolved aerosol volatility measurements from two megacity field studies, Atmospheric Chemistry and Physics, 9, 7161-7182, doi:10.5194/acp-9-7161-2009, 2009.

Jacobson, M. Z.: Isolating nitrated and aromatic aerosols and nitrated aromatic gases as sources of ultraviolet light absorption, Journal of Geophysical Research-Atmospheres, 104, 3527-3542, doi:10.1029/1998jd100054, 1999.

Jimenez, J. L., Canagaratna, M. R., Donahue, N. M., Prevot, A. S. H., Zhang, Q., Kroll, J. H., DeCarlo, P. F., Allan, J. D., Coe, H., Ng, N. L., Aiken, A. C., Docherty, K. S., Ulbrich, I. M., Grieshop, A. P., Robinson, A. L., Duplissy, J., Smith, J. D., Wilson, K. R., Lanz, V. A., Hueglin, C., Sun, Y. L., Tian, J., Laaksonen, A., Raatikainen, T., Rautiainen, J., Vaattovaara, P., Ehn, M., Kulmala, M., Tomlinson, J. M., Collins, D. R., Cubison, M. J., Dunlea, E. J., Huffman, J. A., Onasch, T. B., Alfarra, M. R., Williams, P. I., Bower, K., Kondo, Y., Schneider, J., Drewnick, F., Borrmann, S., Weimer, S., Demerjian, K., Salcedo, D., Cottrell, L., Griffin, R., Takami, A., Miyoshi, T., Hatakeyama, S., Shimono, A., Sun, J. Y., Zhang, Y. M., Dzepina, K., Kimmel, J. R., Sueper, D., Jayne, J. T., Herndon, S. C., Trimborn, A. M., Williams, L. R., Wood, E. C., Middlebrook, A. M., Kolb, C. E., Baltensperger, U., and Worsnop, D. R.: Evolution of Organic Aerosols in the Atmosphere, Science, 326, 1525-1529, doi:10.1126/science.1180353, 2009.

Keyte, I. J., Albinet, A., and Harrison, R. M.: On-road traffic emissions of polycyclic aromatic hydrocarbons and their oxy- and nitro-derivative compounds measured in road tunnel environments, Science of the Total Environment, 566, 1131-1142, doi:10.1016/j.scitotenv.2016.05.152, 2016.

Laborde, M., Schnaiter, M., Linke, C., Saathoff, H., Naumann, K. H., Moehler, O., Berlenz, S., Wagner, U., Taylor, J. W., Liu, D., Flynn, M., Allan, J. D., Coe, H., Heimerl, K., Dahlkoetter, F., Weinzierl, B., Wollny, A. G., Zanatta, M., Cozic, J., Laj, P., Hitzenberger, R., Schwarz, J. P., and Gysel, M.: Single Particle Soot Photometer intercomparison at the AIDA chamber, Atmospheric Measurement Techniques, 5, 3077-3097, doi:10.5194/amt-5-3077-2012, 2012.

Laskin, A., Laskin, J., and Nizkorodov, S. A.: Chemistry of Atmospheric Brown Carbon, Chemical Reviews, 115, 4335-4382, doi:10.1021/cr5006167, 2015.

Liebmann, J., Sobanski, N., Schuladen, J., Karu, E., Hellen, H., Hakola, H., Zha, Q., Ehn, M., Riva, M., Heikkinen, L., Williams, J., Fischer, H., Lelieyeld, J., and Crowley, J. N.: Alkyl nitrates in the boreal forest: formation via the NO3-, OH- and O-3-induced oxidation of biogenic volatile organic compounds and ambient lifetimes, Atmospheric Chemistry and Physics, 19, 10391-10403, doi:10.5194/acp-19-10391-2019, 2019.

Lin, P., Liu, J., Shilling, J. E., Kathmann, S. M., Laskin, J., and Laskin, A.: Molecular characterization of brown carbon (BrC) chromophores in secondary organic aerosol generated from photo-oxidation of toluene, Physical Chemistry Chemical Physics, 17, 23312-23325, doi:10.1039/c5cp02563j, 2015.

Liu, D., He, C., Schwarz, J. P., and Wang, X.: Lifecycle of light-absorbing carbonaceous aerosols in the atmosphere, npj Climate and Atmospheric Science, 3, 40, doi:10.1038/s41612-020-00145-8, 2020.

Liu, D., Taylor, J. W., Young, D. E., Flynn, M. J., Coe, H., and Allan, J. D.: The effect of complex black carbon microphysics on the determination of the optical properties of brown carbon, Geophysical Research Letters, 42, 613-619, doi:10.1002/2014gl062443, 2015a.

Liu, D., Allan, J. D., Young, D. E., Coe, H., Beddows, D., Fleming, Z. L., Flynn, M. J., Gallagher, M. W., Harrison, R. M., Lee, J., Prevot, A. S. H., Taylor, J. W., Yin, J., Williams, P. I., and Zotter, P.: Size distribution, mixing state and source apportionment of black carbon aerosol in London during wintertime, Atmospheric Chemistry and Physics, 14, 10061-10084, doi:10.5194/acp-14-10061-2014, 2014.

Liu, D., Joshi, R., Wang, J., Yu, C., Allan, J. D., Coe, H., Flynn, M. J., Xie, C., Lee, J., Squires, F., Kotthaus, S., Grimmond, S., Ge, X., Sun, Y., and Fu, P.: Contrasting physical properties of black carbon in urban Beijing between winter and summer, Atmos. Chem. Phys., 19, 6749-6769, doi:10.5194/acp-19-6749-2019, 2019a.

Liu, D., Joshi, R., Wang, J., Yu, C., Allan, J. D., Coe, H., Flynn, M. J., Xie, C., Lee, J., Squires, F., Kotthaus, S., Grimmond, S., Ge, X., Sun, Y., and Fu, P.: Contrasting physical properties of black carbon in urban Beijing between winter and summer, Atmospheric Chemistry and Physics, 19, 6749-6769, doi:10.5194/acp-19-6749-2019, 2019b.

Liu, D., Li, S., Hu, D., Kong, S., Cheng, Y., Wu, Y., Ding, S., Hu, K., Zheng, S., Yan, Q., Zheng, H., Zhao, D., Tian, P., Ye, J., Huang, M., and Ding, D.: Evolution of Aerosol Optical Properties from Wood Smoke in Real Atmosphere Influenced by Burning Phase and Solar Radiation, Environmental Science & Technology, 55, 5677-5688, doi:10.1021/acs.est.0c07569, 2021.

Liu, F., Zhang, Q., Tong, D., Zheng, B., Li, M., Huo, H., and He, K. B.: High-resolution inventory of technologies, activities, and emissions of coal-fired power plants in China from 1990 to 2010, Atmospheric Chemistry and Physics, 15, 13299-13317, doi:10.5194/acp-15-13299-2015, 2015b.

Liu, J., Mauzerall, D. L., Chen, Q., Zhang, Q., Song, Y., Peng, W., Klimont, Z., Qiu, X., Zhang, S., Hu, M., Lin, W., Smith, K. R., and Zhu, T.: Air pollutant emissions from Chinese households: A major and underappreciated ambient pollution source, Proceedings of the National Academy of Sciences of the United States of America, 113, 7756-7761, doi:10.1073/pnas.1604537113, 2016.

Liu, P. F., Abdelmalki, N., Hung, H. M., Wang, Y., Brune, W. H., and Martin, S. T.: Ultraviolet and visible complex refractive indices of secondary organic material produced by photooxidation of the aromatic compounds toluene and m-xylene, Atmospheric Chemistry and Physics, 15, 1435-1446, doi:10.5194/acp-15-1435-2015, 2015c.

Makra, L., Matyasovszky, I., Guba, Z., Karatzas, K., and Anttila, P.: Monitoring the long-range transport effects on urban PM10 levels using 3D clusters of backward trajectories, Atmospheric Environment, 45, 2630-2641, doi:10.1016/j.atmosenv.2011.02.068, 2011.

Mohr, C., DeCarlo, P. F., Heringa, M. F., Chirico, R., Slowik, J. G., Richter, R., Reche, C., Alastuey, A., Querol, X., Seco, R., Penuelas, J., Jimenez, J. L., Crippa, M., Zimmermann, R., Baltensperger, U., and Prevot, A. S. H.: Identification and quantification of organic aerosol from cooking and other sources in Barcelona using aerosol mass spectrometer data, Atmospheric Chemistry and Physics, 12, 1649-1665, doi:10.5194/acp-12-1649-2012, 2012.

Nakayama, T., Sato, K., Matsumi, Y., Imamura, T., Yamazaki, A., and Uchiyama, A.: Wavelength and NOx dependent complex refractive index of SOAs generated from the photooxidation of toluene, Atmospheric Chemistry and Physics, 13, 531-545, doi:10.5194/acp-13-531-2013, 2013.

Ng, N. L., Kwan, A. J., Surratt, J. D., Chan, A. W. H., Chhabra, P. S., Sorooshian, A., Pye, H. O. T., Crounse, J. D., Wennberg,

P. O., Flagan, R. C., and Seinfeld, J. H.: Secondary organic aerosol (SOA) formation from reaction of isoprene with nitrate radicals (NO3), Atmospheric Chemistry and Physics, 8, 4117-4140, doi:10.5194/acp-8-4117-2008, 2008.

Paatero, P. and Tapper, U.: POSITIVE MATRIX FACTORIZATION - A NONNEGATIVE FACTOR MODEL WITH OPTIMAL UTILIZATION OF ERROR-ESTIMATES OF DATA VALUES, Environmetrics, 5, 111-126, doi:10.1002/env.3170050203, 1994.

Rizzo, L. V., Artaxo, P., Mueller, T., Wiedensohler, A., Paixao, M., Cirino, G. G., Arana, A., Swietlicki, E., Roldin, P., Fors, E. O., Wiedemann, K. T., Leal, L. S. M., and Kulmala, M.: Long term measurements of aerosol optical properties at a primary forest site in Amazonia, Atmospheric Chemistry and Physics, 13, 2391-2413, doi:10.5194/acp-13-2391-2013, 2013.

Rollins, A. W., Browne, E. C., Min, K. E., Pusede, S. E., Wooldridge, P. J., Gentner, D. R., Goldstein, A. H., Liu, S., Day, D. A., Russell, L. M., and Cohen, R. C.: Evidence for NOx Control over Nighttime SOA Formation, Science, 337, 1210-1212, doi:10.1126/science.1221520, 2012.

Saleh, R., Robinson, E. S., Tkacik, D. S., Ahern, A. T., Liu, S., Aiken, A. C., Sullivan, R. C., Presto, A. A., Dubey, M. K., Yokelson, R. J., Donahue, N. M., and Robinson, A. L.: Brownness of organics in aerosols from biomass burning linked to their black carbon content, Nature Geoscience, 7, 647-650, doi:10.1038/ngeo2220, 2014.

Schuetzle, D.: SAMPLING OF VEHICLE EMISSIONS FOR CHEMICAL-ANALYSIS AND BIOLOGICAL TESTING, Environmental Health Perspectives, 47, 65-80, doi:10.2307/3429500, 1983.

Shen, G., Ru, M., Du, W., Zhu, X., Zhong, Q., Chen, Y., Shen, H., Yun, X., Meng, W., Liu, J., Cheng, H., Hu, J., Guan, D., and Tao, S.: Impacts of air pollutants from rural Chinese households under the rapid residential energy transition, Nature Communications, 10, doi:10.1038/s41467-019-11453-w, 2019.

Siemens, K., Morales, A., He, Q., Li, C., Hettiyadura, A. P. S., Rudich, Y., and Laskin, A.: Molecular Analysis of Secondary Brown Carbon Produced from the Photooxidation of Naphthalene, Environmental science & technology, 56, 3340-3353, doi:10.1021/acs.est.1c03135, 2022.

Sun, Y., Jiang, Q., Wang, Z., Fu, P., Li, J., Yang, T., and Yin, Y.: Investigation of the sources and evolution processes of severe haze pollution in Beijing in January 2013, Journal of Geophysical Research-Atmospheres, 119, 4380-4398, doi:10.1002/2014jd021641, 2014.

Sun, Y. L., Zhang, Q., Schwab, J. J., Demerjian, K. L., Chen, W. N., Bae, M. S., Hung, H. M., Hogrefe, O., Frank, B., Rattigan, O. V., and Lin, Y. C.: Characterization of the sources and processes of organic and inorganic aerosols in New York city with a high-resolution time-of-flight aerosol mass apectrometer, Atmospheric Chemistry and Physics, 11, 1581-1602, doi:10.5194/acp-11-1581-2011, 2011.

Taylor, J. W., Allan, J. D., Liu, D., Flynn, M., Weber, R., Zhang, X., Lefer, B. L., Grossberg, N., Flynn, J., and Coe, H.: Assessment of the sensitivity of core/shell parameters derived using the single-particle soot photometer to density and refractive index, Atmospheric Measurement Techniques, 8, 1701-1718, doi:10.5194/amt-8-1701-2015, 2015.

Tian, P., Liu, D., Zhao, D., Yu, C., Liu, Q., Huang, M., Deng, Z., Ran, L., Wu, Y., Ding, S., Hu, K., Zhao, G., Zhao, C., and Ding, D.: In situ vertical characteristics of optical properties and heating rates of aerosol over Beijing, Atmospheric Chemistry

and Physics, 20, 2603-2622, doi:10.5194/acp-20-2603-2020, 2020.

Ulbrich, I. M., Canagaratna, M. R., Zhang, Q., Worsnop, D. R., and Jimenez, J. L.: Interpretation of organic components from Positive Matrix Factorization of aerosol mass spectrometric data, Atmospheric Chemistry and Physics, 9, 2891-2918, doi:10.5194/acp-9-2891-2009, 2009.

Updyke, K. M., Nguyen, T. B., and Nizkorodov, S. A.: Formation of brown carbon via reactions of ammonia with secondary organic aerosols from biogenic and anthropogenic precursors, Atmospheric Environment, 63, 22-31, doi:10.1016/j.atmosenv.2012.09.012, 2012.

Wang, Q., Han, Y., Ye, J., Liu, S., Pongpiachan, S., Zhang, N., Han, Y., Tian, J., Wu, C., Long, X., Zhang, Q., Zhang, W., Zhao, Z., and Cao, J.: High Contribution of Secondary Brown Carbon to Aerosol Light Absorption in the Southeastern Margin of Tibetan Plateau, Geophysical Research Letters, 46, 4962-4970, doi:10.1029/2019gl082731, 2019a.

Wang, Q., Cao, J., Han, Y., Tian, J., Zhang, Y., Pongpiachan, S., Zhang, Y., Li, L., Niu, X., Shen, Z., Zhao, Z., Tipmanee, D., Bunsomboonsakul, S., Chen, Y., and Sun, J.: Enhanced light absorption due to the mixing state of black carbon in fresh biomass burning emissions, Atmospheric Environment, 180, 184-191, doi:10.1016/j.atmosenv.2018.02.049, 2018.

Wang, X., Heald, C. L., Ridley, D. A., Schwarz, J. P., Spackman, J. R., Perring, A. E., Coe, H., Liu, D., and Clarke, A. D.: Exploiting simultaneous observational constraints on mass and absorption to estimate the global direct radiative forcing of black carbon and brown carbon, Atmospheric Chemistry and Physics, 14, 10989-11010, doi:10.5194/acp-14-10989-2014, 2014.

Wang, Y., Hu, M., Wang, Y., Zheng, J., Shang, D., Yang, Y., Liu, Y., Li, X., Tang, R., Zhu, W., Du, Z., Wu, Y., Guo, S., Wu, Z., Lou, S., Hallquist, M., and Yu, J. Z.: The formation of nitro-aromatic compounds under high NOx and anthropogenic VOC conditions in urban Beijing, China, Atmospheric Chemistry and Physics, 19, 7649-7665, doi:10.5194/acp-19-7649-2019, 2019b.

Wu, C. and Yu, J. Z.: Determination of primary combustion source organic carbon-to-elemental carbon (OCaEuro-/aEuro-EC) ratio using ambient OC and EC measurements: secondary OC-EC correlation minimization method, Atmospheric Chemistry and Physics, 16, 5453-5465, 10.5194/acp-16-5453-2016, 2016.

Yang, W., Zhang, Y., Wang, X., Li, S., Zhu, M., Yu, Q., Li, G., Huang, Z., Zhang, H., Wu, Z., Song, W., Tan, J., and Shao, M.: Volatile organic compounds at a rural site in Beijing: influence of temporary emission control and wintertime heating, Atmospheric Chemistry and Physics, 18, 12663-12682, doi:10.5194/acp-18-12663-2018, 2018.

Yao, Z., Shen, X., Ye, Y., Cao, X., Jiang, X., Zhang, Y., and He, K.: On-road emission characteristics of VOCs from diesel trucks in Beijing, China, Atmospheric Environment, 103, 87-93, doi:10.1016/j.atmosenv.2014.12.028, 2015.

Zhang, Q., Jimenez, J. L., Canagaratna, M. R., Ulbrich, I. M., Ng, N. L., Worsnop, D. R., and Sun, Y.: Understanding atmospheric organic aerosols via factor analysis of aerosol mass spectrometry: a review, Analytical and Bioanalytical Chemistry, 401, 3045-3067, doi:10.1007/s00216-011-5355-y, 2011.

Zhang, Y., Zhang, Q., Cheng, Y., Su, H., Li, H., Li, M., Zhang, X., Ding, A., and He, K.: Amplification of light absorption of black carbon associated with air pollution, Atmospheric Chemistry and Physics, 18, 9879-9896, doi:10.5194/acp-18-9879-2018, 2018.

https://doi.org/10.5194/acp-2022-483
Preprint. Discussion started: 18 July 2022

Atmospheric Chemistry and Physics Discussions

Zhao, R., Lee, A. K. Y., Huang, L., Li, X., Yang, F., and Abbatt, J. P. D.: Photochemical processing of aqueous atmospheric brown carbon, Atmospheric Chemistry and Physics, 15, 6087-6100, doi:10.5194/acp-15-6087-2015, 2015.